Current Biology, Vol. 13, R721–R733, September 16, 2003, ©2003 Elsevier Science Ltd. All rights reserved. DOI 10.1016/S0960-9822(03)00652-3

Polymer Motors: Pushing out the Front and Pulling up the Back

Review

Alex Mogilner[1] and George Oster[2]

Mechanical work in cells is performed by specialized motor proteins that operate in a continuous mechanochemical cycle. Less complex, but still efficient, 'one-shot' motors evolved based on the assembly and disassembly of polymers. We review the mechanisms of pushing and pulling by actin and microtubule filaments and the organizational principles of actin networks. We show how these polymer force generators are used for the propulsion of intracellular pathogens, protrusion of lamellipodia and mitotic movements. We discuss several examples of cellular forces generated by the assembly and disassembly of polymer gels.

Introduction

More than 20 years ago, Abercrombie noted that crawling cells move in three stages [1,2]. First, they push out their leading edge; then they strengthen their adhesions at the leading edge and weaken them at the trailing edge; finally, they pull up their rear. Protrusion involves generating pushing forces at the front, and pulling up the back involves contractile forces. Successes in cell biology, genetics, biophysics and modeling over the past few decades have dissected the cell migration phenomena so that the process appears less mysterious than it did in Abercrombie's day [3]. Many molecular details remain vague, however, leaving questions unanswered and hypotheses unconfirmed. Here we discuss but one aspect of cell migration: the physical origins of the forces that drive cell movements. Broader and more particular aspects of cell motility are discussed in several recent reviews and books [2,4–10].

The first things that comes to mind when discussing force generation are the motor proteins that convert the chemical energy of nucleotide hydrolysis into mechanical work [11,12]. Myosin motors drive contraction of actin networks, and kinesin and dynein motors transport organelles and vesicles along microtubules. These molecular motors have evolved mechanochemical cycles that enable them to move at hundreds of nanometers per second along their polymer tracks and, if stalled, generate forces in the range of piconewtons (pN). There are many other hydrolysis-driven protein motors that are not involved in cell motility (see, for example, [13]). In this review, we shall focus on much simpler force generators that may have appeared earlier during evolution. Rather than using complex allosteric conformational changes, these motors rely on the relatively simpler processes of polymerization and depolymerization of dynamic biopolymers and on the gelation and solation of cytoskeletal gels. These motors do not operate in a cyclic fashion, undergoing a number of steps that correspond to changes in conformation and in chemical state and eventually resetting themselves to their initial configuration. Rather, they are 'one-shot' engines that do their increment of work and then are disassembled and reassembled at another place in the cell.

[1]Department of Mathematics and Center for Genetics and Development, University of California, Davis, California 95616, USA. E-mail: mogilner@math.ucdavis.edu [2]Departments of Molecular & Cellular Biology and ESPM, University of California, Berkeley, California 94720-3112, USA. E-mail: goster@nature.berkeley.edu

How Individual Filaments Push

All molecular motors work on the same general principle: short-range molecular attractions capture 'favorable' Brownian fluctuations (see Box 1 and [12–14]). How they accomplish this depends on their protein geometry, the diversity of which gives rise to the wide variety of protein motors. Unlike most protein motors, the filament motors we discuss here have a comparatively simple geometry and so their principle of operation is fairly well understood.

Hill and Kirschner [15] used thermodynamics to demonstrate that a polymerizing filament would not necessarily stop growing when it runs into an obstacle. Rather, the resistance from the obstacle would slow its growth, thus demonstrating that polymerization can generate a force. Subsequently, actin polymerization was observed to develop enough force to deform lipid vesicles [16–18], suggesting that actin polymerization may be responsible for pushing out the front of motile cells [19].

The thermodynamic approach had severe limitations, for it says nothing about the molecular mechanism, and tells only what force *could* be generated in the limit of very slow ('quasi-static') polymerization rates when the system is very close to equilibrium, which is not the case in a live cell. A mechanistic theory was needed to compute the force actually generated under cellular conditions. Macroscopically, the mechanism by which polymerization can generate force is not obvious, for it would appear that, when a growing filament's tip 'bumps' into an object, the growth would simply cease because there is no room between the tip and the object for a monomer to squeeze in. The key difference on the molecular scale is Brownian motion.

Peskin *et al.* [20] formulated a mechanistic theory to account for the force generated by polymerization when the polymers are rigid. They called this model the 'Brownian ratchet' to distinguish it from the 'ratchet and pawl' model famously discussed by Feynman [21] to illustrate the thermodynamic impossibility of obtaining work from an *isolated* isothermal system. Because they are small, cells are isothermal, but they are not isolated, and they contain abundant energy sources.

Box 1

The Polymerization Ratchet

Proteins convert thermal fluctuations into mechanical force in a variety of ways. However, two prototypical strategies are generally referred to as *power strokes* and *Brownian ratchets* [12,22,106]. In a power stroke, the binding reaction is mechanically coupled to movement and generation of force. For example, if the chemical reaction of a monomer binding to a filament tip triggered a conformational change in the monomer that elongated it, then such 'stroke' would directly drive an object in front of the polymer tip. In a Brownian ratchet, the role of monomer binding reaction is to prevent backward fluctuations of the load, rather than to apply a mechanical force directly to it (Figure 1). That is, the load is driven by its own Brownian fluctuations, and the chemistry provides the energy to rectify its diffusive motion [11,12].

This nomenclature is somewhat misleading, as the two mechanisms represent extreme cases; another viewpoint can make this clear. If we picture the advancement of a protein motor as moving down on a bumpy free energy landscape (Figure 1), a power stroke is an inclined path with bumps only a few k_BT high, where $k_BT \approx 4.1$ pN·nm is the 'unit' of thermal energy, k_B being Boltzmann's constant and T the absolute temperature [8]. A ratchet potential energy has a 'staircase' profile with step heights much larger than k_BT, as shown in Figure 1. The object diffuses uphill against the load force until it reaches the vertical drop that represents the monomer binding step. Once bound, the new monomer must surmount a large energy barrier to be dislodged, and so backward diffusion is very unlikely; thus, work is done against the load force because the chemical step is nearly irreversible. This example clearly illustrates how chemical energy is expended to preferentially select forward steps (or prevent backward steps) and hence to favor forward motion. It also illustrates that the difference between ratchets and power strokes is only a matter of degree: a power stroke biases thermal motion by a sequence of small free energy drops, while a ratchet rectifies diffusion by a sequence of large free energy changes. For a detailed discussion of the forces generated by single motor proteins see [12,22,107].

The simplest way to convert chemical energy into a mechanical force is by polymerizing a filament against a load force, F_L, using the free energy of binding of a monomer onto the tip of the polymer, ΔG_b. If the polymer assembly is unobstructed, its elongation rate is simply $V_p = \delta(k_{on}M - k_{off})$ where δ [nm] is the size of the monomer, M [μM] the monomer concentration, and k_{on} [1/(μM sec)], k_{off} [1/sec] are the polymerization and depolymerization rate constants, respectively. Now suppose an object, say a small sphere, is aligned ahead of the growing polymer that is anchored at its left end (see Figure 1). The polymer does not actually 'push' the object, but it can 'rectify' its Brownian motion as follows. Assume that the polymer is perfectly rigid, and that the sphere has a diffusion coefficient, D. In order for a monomer to bind to the end of the filament the object must open up a gap of size δ by diffusing away from the tip, and remaining there for a time ~$1/k_{on}M$ to allow a polymerization event to take place. In the limiting case when diffusion is much faster than polymerization, that is, $k_{on}M << D/\delta^2$, the elongation rate is given by the simple formula $V_p = \delta(k_{on}M \cdot p(\delta, F_L) - k_{off})$. That is, the polymerization rate is weighted by the probability $p(\delta,F_L)$ that the gap size is δ or larger [20,23]. This probability depends on the load force F_L pushing the object to the left; in this simple case $p = \exp[-F_L\delta/k_BT]$, where $F_L\delta$ is the work done required to move the object a distance δ.

We can picture the situation as a point moving on a free energy landscape, as shown in Figure 1. The object diffuses 'uphill' against the load force on a 'staircase' free energy function, each with a step height equal to the monomer binding free energy. The stall load, F_{stall}, is reached when the work done in moving the object a distance δ is just equal to the free energy of the binding reaction; that is, $V = 0$ when the load force is $F_{stall} = (k_BT/\delta)\ln(k_{on}M/k_{off})$, which corresponds to the equilibrium thermodynamic expression. In the case of actin polymerization, M is usually in the micromolar range, the polymerization rate is $k_{on}M$ ~100/sec, and the depolymerization rate is k_{off} ~1/s, and each monomer added to the polymer tip increases its length by $\delta \approx 2.7$ nm. Therefore, without significant load, $V_p \approx 0.1$–1 μm/s. When stalled, a filament generates force of ~5–7 pN, similar to that generated by myosin and kinesin [108,109]. These estimates work in the limit when the object's diffusion is very fast, which is not always the case. As explained in the text, however, actin filaments are not rigid, and their thermal bending undulations are very fast (~10^4/s). The analysis in this case is similar, and it turns out that the above expression for the stall force is still valid [23].

The filament length is another important factor. The effective elastic constant of an actin filament of length L tilted at angle θ to an obstacle is $k \approx 4\lambda k_BT/(L^3\sin^2(\theta))$ [23], where λ is the persistence length, which is in micron range [94]. This formula indicates that if the filament is too short (less than ~70 nm), or the angle θ is too acute (less than ~30°), the filament is effectively too stiff for the elastic ratchet to work; that is, thermal fluctuations are insufficient to create a gap large enough for intercalation. On the other hand, if the filament is too long, it becomes too 'soft', and it buckles under a sub-piconewton force.

For microtubule polymerization, the mathematics is more involved [25,30]. If all 13 microtubule proto-filaments are considered as independent force generators, 'subsidizing' each other as described in the text, then the theoretically predicted stall force is $F_{stall} \approx 7$ pN (for relevant parameters, see [25,30]).

Polymerization motors are simple and reliable, and in terms of energy consumption they are moderately efficient. Indeed, the efficiency, η, can be estimated from the ratio of the work performed, $F_L \cdot \delta$, to the monomer binding free energy:

$\Delta G_B = k_BT\ln(k_{on}M/k_{off}) = 4.1$[pN·nm] $\ln(11.6$ [μM/s]·10 [μM])/(1 [1/s]) ≈ 20 [pN·nm]. Thus $\eta = 5$ [pN]·2.7 [nm]/20 [pN·nm] ≈ 0.68. However, there is a large cost associated with controlling when and where polymerization occurs in the cell. This control depends on the hydrolytic activity of actin, for each monomer of actin binds and hydrolyzes one ATP molecule, whose free energy of hydrolysis is ~80 pN·nm. Comparing this to the work performed in a step gives a 'control' efficiency of only η_c ~15%. For a microtubule, the energy of hydrolysis ~26 pN·nm per dimer is used to generate ~7 pN·(8/13) nm of work, so the control efficiency is again ~15%. (GTP hydrolysis eventually allows for the generation of pulling force, but this is a separate efficiency.) When polymerization is fast, η_c drops below 10% far from stall.

The ratchet model can be used to estimate the forces generated by the depolymerizing microtubule in the model proposed by Peskin *et al.* [49] where a bead (or docking motor) diffusively rolls without dissociation on the microtubule and facilitates depolymerization when it is near the tip. In this model, a large force keeps the bead near the microtubule end (but the motor does not come off end) so that dimers disassemble from the tip with rate k_{off}. Each disassembly event allows the motor to rotate a little toward the minus end of the microtubule. However, the resulting step is much smaller than the size of the dimer. The step's size, δ, is determined by the thermal energy required for the step against the load force, F_L: $F_L \cdot \delta = k_BT$ or $\delta \approx k_BT/F_L$. Thus $V_p \approx k_{off}\delta = k_{off}k_BT/F_L$. Therefore, the depolymerization velocity decreases inversely proportional to the load force. According to this formula the depolymerization can never reach zero; in reality, a large force would break the bonds between the docking motor and the microtubule end. However, at a load force a few fold greater than k_BT/δ, depolymerization would slow down significantly. Thus this depolymerization motor can develop force only in the pN range.

So extracting work from an isothermal environment poses no problem for the second law of thermodynamics [12,22]. According to this model, an object in front of the filament diffuses away from the tip, creating a gap sufficient for monomers to intercalate and assemble onto the tip, thereby inhibiting the object from diffusing backward. Even when a resisting load force is applied to the object, Brownian motion can still create a sufficient gap, and so the object's diffusion is biased forward. This 'ratcheting' of diffusive motion can generate force in the pN range (Box 1). If the polymer is not rigid, its own thermal undulations can create a gap between its tip and the load [23]. If the gap is large enough and persists long enough, a monomer can intercalate into the gap and bind onto the tip of the growing polymer. This increases the fiber's length so that, when the tip contacts the load, the polymer is bent and the resulting elastic force pushes on the load. In general, both filament and load are fluctuating, and the combined effect can be sufficient to allow intercalation of monomers and consequent force generation. This 'elastic ratchet' model is sufficient to explain the forces developed by polymerizing actin and microtubule filaments [23–26].

Actin is a 43 kDa globular protein that polymerizes into a linear, two-stranded and right-handed double helix which twists around itself every 37 nm. Each monomer is ~5.4 nm in size, so that assembly of a monomer imparts a 2.7 nm axial rise to the filament. Both strands of the helix have the same polarity, so the two ends of the filament are structurally different: they are termed barbed and pointed ends because of their appearance when decorated with myosin. The barbed end assembles and disassembles monomers at a rate two orders of magnitude faster than the pointed end. In the absence of nucleotide hydrolysis, the critical concentration of monomeric actin — when the rates of polymerization and depolymerization balance — is the same at both ends. At this concentration, the average length and position of a filament do not change [8,27].

Actin monomers bind ATP, however, and the filaments they polymerize into become dynamically asymmetric. The structural details accompanying ATP hydrolysis are not known, but it produces an asymmetry at the two filaments ends. As a result of this asymmetry, the effective affinity for new monomers at the barbed end is high and the critical concentration is low, ~0.2 μM. At the pointed end, the monomer affinity is low, so that the corresponding critical concentration is higher, ~0.7 μM. The consequence of this asymmetry is the non-equilibrium process of 'treadmilling': net depolymerization from the pointed end balanced by net polymerization onto the barbed end without changing its average length. But *the center of mass of the polymer remains stationary, as no external force is acting on it*. Monomers simply recycle by diffusion, which is biased by preferential binding at the barbed end and unbinding at the pointed end. So treadmilling consumes chemical energy via hydrolysis, but this is a *kinematic* phenomenon that does not generate any force.

The energy source for production of force is the binding free energy of monomers to the polymer tip. This binding energy is used to rectify the Brownian motion of the load against which the polymer is pushing (Box 1). More precisely, the force is generated by thermal fluctuations of the *load*, and the binding free energy is used to rectify its thermal displacements. The *proximal* role of ATP hydrolysis is to control the rate and location of polymerization, not force production. Thus, like many energy conversions in the cell, the polymerization motor 'borrows' energy in various forms and stores it for later use. That actin filaments can push *in vitro* has been confirmed experimentally [28]. Its relevance to pushing out the front of the cell *in vivo* is discussed below.

Because F-actin is rather fragile, the force–velocity relation for a single actin fiber is difficult to measure. Microtubules are much sturdier filaments, however, and force generation by this polymer has been measured by observing how a single microtubule buckled when polymerizing against a wall [29]. This experiment demonstrated that a microtubule growing at the plus end develops a force of a few pN and that the net polymerization velocity decreases exponentially as a function of the load force in the fashion predicted by the elastic ratchet model (see Box 1 and [25,30]).

Force production by microtubules is more complex than that of actin because microtubules consist of about 13 protofilaments, which do not polymerize independently. Thus, the force generated by the protofilaments is not simply the sum of the individual protofilament forces. The reason is apparent: at any instant, those protofilaments that are too close to the load cannot polymerize very fast because the gaps between their tips and the load are insufficient to allow intercalation of a tubulin dimer. But these protofilaments can 'subsidize' the growth of other protofilaments by supporting a large portion of the load. Analysis of the 'subsidy effect' shows that the force–velocity relation of the growing microtubule is still exponential, in agreement with experiments [25,29,30]. More studies are needed to determine how the growth of the protofilaments influences one another, and to determine the effects of elasticity of the microtubule lattice and GTP hydrolysis on polymerization. As measurements near stall are inaccurate, modeling is especially important.

Experiments with microtubules growing inside liposomes confirm that polymerization of microtubules can generate enough force to deform the membrane [31,32]. The forces developed by microtubule polymerization are capable of driving spindle and chromosome movement during mitosis [33,34]; whether they do so *in vivo* is less clear. For example, in the fission yeast *Schizosaccharomyces pombe*, oppositely directed microtubules are attached to the nucleus by their minus ends. When their plus ends reach the surface of the cell, the polymers push back on the nucleus. This pushing from the two ends of the cell tends to center the nucleus within the cell [35]. Another example is the polar ejection force exerted by growing microtubules on chromosome arms during prometaphase [36]. This force is not likely to depend on microtubule polymerization alone: plus-end-directed kinesin motors are also involved [37]. Finally,

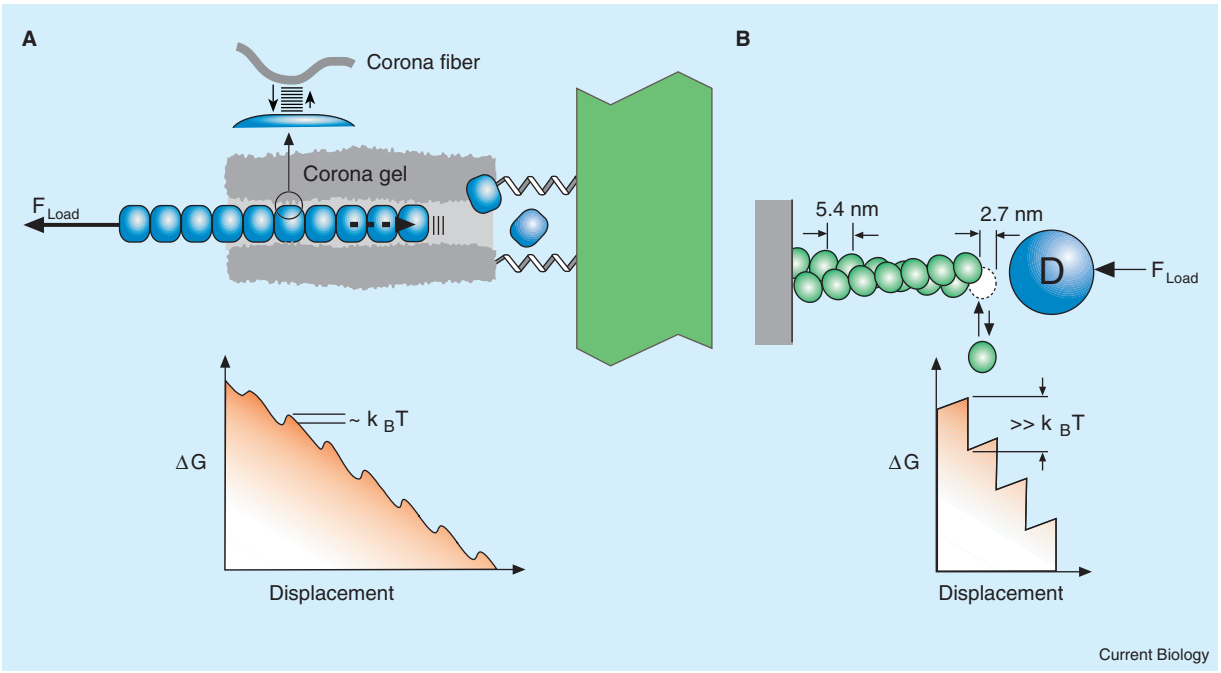

Figure 1. Power strokes and ratchets.
(A) Hypothetical model of pulling force generation at the kinetochore similar to Hill's model [43]. A microtubule (blue) slides into the 'corona fibers' emanating from the kinetochore (green) (reviewed in [110]). The fibers have a moderate affinity for the microtubule. The corresponding binding free energy gradient is shown below. Thermal fluctuations of the fibers 'lubricate' their movement and drive them across the potential barriers arising from breaking the interactions between the fiber and microtubules. If both the barriers and the downward free energy steps are comparable to the thermal energy (k_BT), then the motor is said to generate force by a power stroke mechanism. (B) A perfect polymerization ratchet. A rigid actin filament polymerizes against object fluctuating with diffusion coefficient D. Each time the gap between the filament tip and the object is sufficiently large and persists for a long enough time, a monomer intercalates into the gap and assembles onto the filament tip rectifying object's thermal fluctuations. Each monomer binding drops the free energy significantly, relative to thermal energy. This polymerization motor uses a Brownian ratchet mechanism to generate force since the free energy drop per step is much greater than k_BT, and the motor does not directly drive the load, but simply rectifies its Brownian diffusion.

theoretical studies indicate that polymerization forces can be important in separating centrosomes during early prophase [38].

How Individual Filaments Pull

While polymerizing microtubules can generate a pushing force, depolymerizing microtubules can develop pulling forces, although the mechanism is less obvious. For example, using *in vitro* assays, Coue *et al.* [39] observed that the depolymerizing ends of microtubules can pull particles at rates of almost 1 μm/sec against estimated viscous drag forces of ~10 pN. Subsequently, Lombillo *et al.* [40] found that plastic beads coated with plus-end-directed microtubule motors remain attached to the plus ends of depolymerizing microtubules and are carried toward the microtubule minus ends as the polymer shortens. This work also showed that kinesins can maintain dynamic attachments to the microtubule end even at ATP concentrations that are too low for force production.

Thus, microtubule depolymerization can generate forces sufficient to pull chromosomes to the pole and so motor proteins may not be needed to generate the pulling force. Rather, the motors may function as passive 'docking' proteins to link the depolymerizing polymer end with the cargo. Such docking proteins should have unusual properties: they cannot detach from the plus end, yet they do not block its depolymerization, and may enhance it. For example, the kinesin motor protein XKCM1/MCAK localizes to kinetochores, where it is thought to induce microtubule disassembly [41], whereas the motor protein CENP-E is thought to use its plus-end-directed motor activity to anchor kinetochores to the shortening plus ends of microtubules during anaphase [42]. XKCM1/MCAK motors can induce the shortening of kinetochore-to-pole microtubules during anaphase, and this may work in concert with the plus-end anchoring activity of CENP-E. A plausible hypothesis for how XKCM1/MCAK destabilizes a growing microtubule is that it binds to the bent form of the tubulin near the depolymerizing plus end, imparting an additional stress which weakens the association of the terminal GTP–tubulin dimer and promotes its dissociation [6].

The nature of the pulling force associated with microtubule depolymerization remains elusive. The earliest model by Hill [43] assumed that the tip of the depolymerizing microtubule slides through the hole in a sleeve-like docking protein that allows tubulin dimers to dissociate freely from the microtubule tip (Figure 1A). The interior of this sleeve has a high affinity for the microtubule lattice; consequently when subunits dissociate from the microtubule tip the binding free energy gradient favors deeper insertion of the

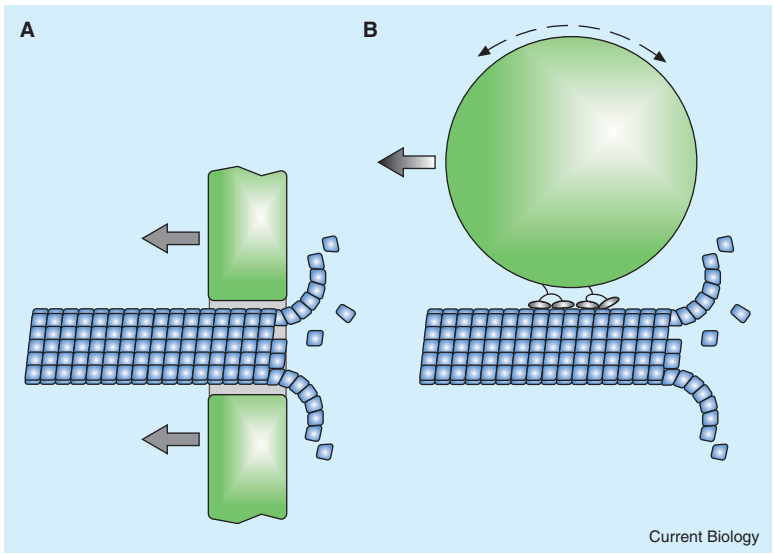

Figure 2. How depolymerizing microtubules can pull.
(A) The 'conformation wave' model of pulling force generation by a depolymerizing microtubule [46]. The elasticity of the protofilaments that curve outward at the disassembling plus end drives a hypothetical sliding collar on the kinetochore toward the minus end, generating force by a power stroke mechanism. (B) A bead coated with tubulin binding proteins undergoes rotational diffusion along the microtubule. The binding free energy gradient prevents the bead from detaching from the plus end of the microtubule and, as it rolls, the bead facilitates depolymerization at the plus end. Rotational diffusion of the bead is ratcheted by the depolymerizing plus end [49].

microtubule into the sleeve. Thus, Brownian motion will drive the docking protein toward the microtubule minus end, producing a pulling force. Repositioning of a microtubule within the sleeve also requires previous interactions to be broken and reformed, posing a potential energy barrier to the movement of the sleeve. This barrier increases with deeper microtubule insertion into the sleeve, which slows further movement of a microtubule. If the rate of tubulin loss is equal to the net rate that the microtubule is drawn into the sleeve, the sleeve will follow the tip of the depolymerizing microtubule with constant average speed.

An important characteristic of Hill's model is that over a wide range of increasing load force, the speed of depolymerization-coupled movement will remain constant [44]. This behavior arises because the steady state force generated by the sleeve adapts to an opposing load by adjusting the average length of the fiber inside the sleeve so that the speed of the load is equal to the depolymerization rate. When the load force is greater than the gradient of the binding free energy, the microtubule is pulled out of the collar completely. This argument predicts an unusual concave force-velocity relation similar to that measured for RNA polymerase [45]. But as it is difficult to connect the model to actual structures the parameters, and thus the magnitude of the generated force, are hard to estimate.

Another possible mechanism is the 'conformation wave' model proposed by Mitchison [46] (Figure 2A). Depolymerizing microtubule ends consist of two-dimensional sheets that appear frayed and curved, often resembling rams' horns [47]. This probably arises because binding GTP to tubulin monomers induces a conformational change that permits polymerization. When GTP is hydrolyzed and the monomer tries to relax to its stress free state, it cannot because it is trapped in the microtubule lattice. Thus the microtubule is in a state of elastic strain that can only be released as the microtubule depolymerizes, as evidenced by the 'banana peel' curvature of the frayed ends [48]. The elasticity of the protofilaments that curve outward at the disassembling plus end can drive a sliding collar toward the minus end (Figure 2A). In this case, the force driving the movement of the sleeve is the release of mechanical strain stored in the lattice during microtubule polymerization. The bending of the protofilament sheets induced by GTP hydrolysis is analogous to the power stroke. This model has not been treated quantitatively, but the force it generates can be estimated knowing the strain energy stored in the microtubule lattice from the GTP hydrolysis: ΔG ~26 pN·nm/dimer [5]. Dividing by the fiber length increment after one act of unbinding gives 26 pN·nm/(8 nm/13) ~45 pN. Thus, this mechanism can generate up to a few tens of pN per microtubule fiber.

Finally, Peskin *et al.* [49,50] developed a quantitative model in which a bead coated with high-affinity tubulin binding proteins undergoes rotational diffusion along the microtubule polymer lattice (Figure 2B). The binding energy gradient prevents the bead from detaching from the plus end of the microtubule, and as it rolls it weakens the bonds between neighboring tubulin dimers and so facilitates depolymerization at the tip. This mechanism is a ratchet: rotational diffusion of the bead is biased by the depolymerizing plus end of the polymer. In Box 1, we estimate that force generated by this mechanism is a few pN, comparable to those generated by kinesin and dynein motors.

As depolymerization forces are likely to play significant roles in driving mitotic movements [51], how much force is actually required to function in mitosis? The viscous drag coefficient of a chromosome in the cytoplasm is ~10 pN·sec/μm, which means that a small force of ~(10 pN·sec/μm) x (0.1 μm/sec) ~1 pN would be sufficient to drag the chromosome [52]. But mitotic microtubules seem to generate much greater forces. Using calibrated flexible glass needles, Nicklas [53] measured the force generated on the kinetochore during anaphase. He discovered that chromosome velocity was not affected until the opposing force reached ~100 pN, and then fell rapidly with increasing force. The stall force was ~700 pN, which is several

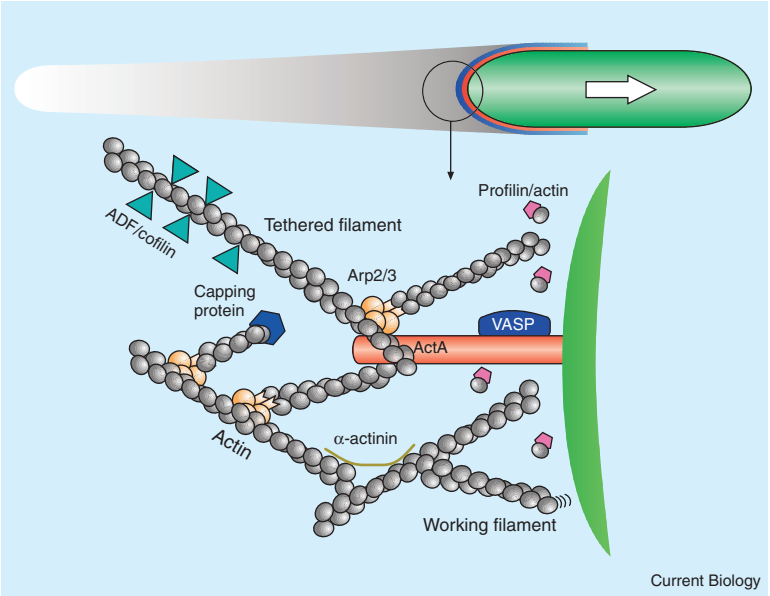

Figure 3. How actin polymerization pushes *Listeria*.
Actin polymerizes at the bacterial surface and disassembles distally causing tail to thin and narrow far from the bacterium. The posterior bacterial surface is coated with ActA which promotes actin polymerization at the surface. The insert shows the molecular machinery at the bacterial surface. ActA assisted by VASP activates Arp2/3 complex and serves as a scaffold for actin assembly. Activated Arp2/3 complex nucleates and branches actin filaments. Efficient actin turnover is regulated by capping proteins that limit filament growth. ADF/cofilin accelerates actin disassembly away from the bacterial surface; profilin sequesters actin monomers and restricts polymerization to the region adjacent to the surface. α-actinin cross-links actin filaments and solidifies the tail. Tethered 'mother' filaments transiently attach to the surface and resist the forward movement of the bacterium. The tethered filaments in tension eventually detach and become 'working' filaments in compression whose thermal undulations exert the propulsive pressure on the bacterial wall [26].

orders of magnitude greater than the calculated value of 1 pN required to overcome viscous drag.

Puzzles abound in mitosis. For example, prior to division in the budding yeast *Saccharomyces cerevisiae*, microtubules growing from one of the spindle poles attach to the cell cortex. The depolymerization of these microtubules is thought to reel in the spindle, which would require quite large forces [54]. It appears that both active and docking motors along with microtubule depolymerization co-operate to generate mitotic forces. Explaining this most central of cell processes is thus still very much an open issue.

How Actin Propels Intracellular Pathogens

Many intracellular pathogens are propelled by the polymerization of actin filaments. This has attracted attention because these pathogens may serve as simplified model systems for eukaryotic cell motility: a purely protrusive system without adhesion, contraction or the added complexity of the eukaryotic cell membrane. In particular, *Listeria monocytogenes* propels itself by assembling the host cell actin into a comet-like tail of cross-linked filaments, with their polymerizing barbed ends oriented toward the bacterial surface [55]. *Listeria* moves through the host cytoplasm rapidly, with velocities of a few tenths of a micron per second [56]. Actin polymerizes at the bacterial surface with the same rate as its velocity, suggesting that actin growth drives the bacterium forward [57]. Only one protein on the surface of *Listeria,* ActA, is required for motility [58]. In addition to actin monomers, ActA and ATP, only a handful of proteins in cytoplasmic extracts are essential for bacterial propulsion, including the nucleating and branching complex, Arp2/3, capping proteins and the severing and depolymerizing factor, ADF/cofilin (Figure 3) [59].

Though still not confirmed in all its details, the *dendritic nucleation model* explains much of the geometrical organization of actin-based propulsion [3,60,61]. ActA activates the Arp2/3 protein complex, which in turn mediates nucleating and branching of the nascent filaments from the sides or tips of the existing actin fibers. Thus the comet-like tail has a branched organization, with Arp2/3 complex localizing to the Y-junctions that give birth to daughter filaments oriented at about 70° to the mother filament. Capping activity terminates elongation of the barbed ends, and ADF/cofilin accelerates filament disassembly, so the tail density decreases exponentially away from the posterior bacterial surface. The VASP protein and the cross-linking protein α-actinin — the latter assisting Arp2/3 complex in weaving short filaments into the tail network — are not essential, but stabilize and accelerate the movement [62,63]. Myosin does not participate in bacterial propulsion, and it is now generally accepted that actin polymerization provides the force for bacterial movement [4], the propulsive force arising from the thermal motions of the polymerizing filament tips (Box 1).

Initially, Peskin *et al.* [20] applied the rigid polymerization ratchet theory to *Listeria* propulsion, considering the cell itself as the thermally fluctuating object in front of the filament tips. This model predicted that the bacterial velocity should depend on its diffusion coefficient, and thereby on its size. Experiments failed to show such a size dependence, and so the elastic polymerization ratchet model was proposed [24]. This model resolved the size independence issue; however, as often happens, another apparently irreconcilable observation arose — the actin tail appeared to be attached to the surface of the cell [56,64,65].

While filament attachment confers stable and persistent movement, how can Brownian ratchet-type models work if the filaments are attached to the

surface? The 'tethered ratchet' model answers this question by assuming that the filaments attach to the bacterial surface transiently [26]. Nascent filaments are associated with the protein complexes on the surface. However, they soon dissociate and grow freely until finally they are capped and lose contact with the surface. During this process, the attached fibers are in tension and resist the forward progress of the bacterium. At the same time, the dissociated fibers are in compression and generate the force of propulsion. Recently, two groups [66,67] measured the force–velocity relations by using methylcellulose to increase the viscosity of the medium in which bacteria move. Though the details of the measurements are different, the experiment indicates that slowing the bacteria requires loads of tens to hundreds of pN. This agrees with the tethered ratchet theory, which predicts that hundreds of 'working filaments' push against tens of attached ones. Additional loads in the hundred pN range would add to the internal resistance of hundreds of pN from the attached filaments and stall the working filaments, each of which develops force of a few pN.

Other intracellular pathogens use *Listeria's modus operandi*: *Shigella*, the spotted fever bacterium *Rickettsia*, and *Vaccinia* virus separately and convergently evolved similar mechanisms to exploit the cellular actin assembly machinery for propulsion [68]. The general mechanism is the same in all these cases, though important molecular details vary. For example, *Shigella* uses the surface protein IcsA instead of ActA to stimulate actin polymerization. *Vaccinia* uses tyrosine phosphorylation of protein A36R, absent in *Listeria* and *Shigella*. *Rickettsia* does not employ Arp2/3 complex as an actin nucleating/branching center — it is not clear what, if any, is the substitute — and so its tail consists of long actin filaments arranged in a parallel array. This array is strikingly different from those of *Listeria*, *Shigella*, or *Vaccinia*, which consist of short filaments cross-linked at acute angles. This diversity of organisms has now been complemented by *in vitro* assays using plastic beads and lipid vesicles which, when coated with either ActA, or WASP proteins, move much the same way as the pathogens. These promise to become useful tools in uncovering the secrets of cell motility (see the review by Upadhyaya and van Oudenaarden in this issue, and [58,69]).

Forces in Lamellipodia

Lamellipodial protrusion is perhaps the most well-studied motility phenomena, and a great deal of molecular details are available [3]. Despite this, there is no agreed scenario that applies to all cell types. There are many similarities between actin dynamics in *Listeria* and in the lamellipodia of some rapidly moving eukaryotic cells, and there is a general consensus that actin polymerization is the lamellipodial motor [60]. The lamellipod is a broad, flat, sheet-like structure, tens of μm in width, and 0.1–0.2 μm thick [70]. Lamellipodial actin filaments form a polarized network; fibers are cross-linked in a nearly square lattice where filaments subtend roughly a 55° angle to the front edge of the cell [71,72].

The reason for this order is the sterically precise branching mediated by Arp2/3 complex that imposes a 70° branching angle between mother and daughter filaments. The growing barbed ends abut the extreme leading edge of the lamellipod while the disassembling pointed ends dominate far from the leading edge. Sequestering proteins shuttle monomers from the back to the front by simple diffusion [73]. Barbed-end capping produces an excess of free pointed ends. This keeps the supply of monomers plentiful and accelerates growth of any barbed ends that are temporarily uncapped [61]. The actin network advances by *array treadmilling*, rather than by treadmilling of individual filaments [3]. Barbed ends of a few filaments grow at the leading edge, while their pointed ends are stable; other filaments have both ends capped, and yet others have the barbed ends capped and the pointed ends depolymerizing.

Accurate measurements of the force of lamellipodial protrusion are not available. Experimental estimates of the force developed by 1 μm of the leading edge are ~1000 pN (reviewed in [74]). As there are hundreds of actin fibers per μm of leading edge, this is consistent with the elastic ratchet model that predicts that each filament generates a few pN [70]. When not stalled, the actin easily overcomes the resistance of tens of pN required to bend the cell membrane [75], and the hundreds of pN required to break the attachments between the actin cortex and cell membrane [76]. The optimal angle between filaments and the direction of protrusion predicted by the theory, ~30–60°, is observed [71].

Statistical analysis and modeling of light microscopic images suggest that actin filament lengths are between a few hundred nm and 1 μm (A. Verkhovsky, personal communication), which is in a similar range to the predictions of the elastic polymerization ratchet model for optimal filament length. Moreover, lamellipodia with excess Ena/VASP contain longer filaments. These often contract, apparently because long, flexible actin filaments buckle easily [77]. Despite our qualitative understanding of *Listeria* and lamellipodial protrusion, significant pieces of the puzzle are missing. For example, it appears that local osmotic forces also play a role in protrusion (see below), so the elastic polymerization ratchet drive may not be the only actor on the leading edge stage.

Other Mechanisms of Force Generation

There are alternative proposals to the elastic ratchet model for polymerization force generation. Generally, they fall into two categories: hypothetical protein motors and macroscopic phenomenological models. An example of the former is the molecular ratchet motor proposed by Laurent *et al.* [78] which posits that frequent attachment and detachment of VASP on the cell surface to F-actin allows it to slide along a growing filament, driven by the free energy of monomer addition. Another example of an hypothetical force generator is an affinity-modulated, clamped-filament elongation mechanism that exploits actin's intrinsic ATPase activity [79].

Kuo and McGrath [65] observed that *Listeria* appeared to advance in discrete steps of 5.5 nm, similar

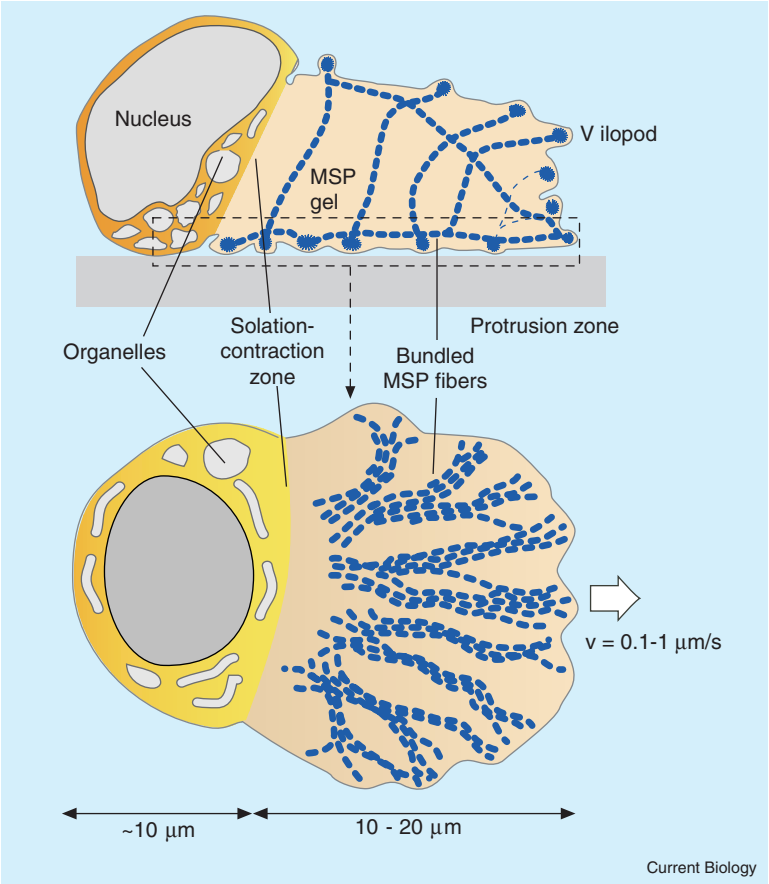

Figure 4. The 'push-pull' model of locomotion of the nematode sperm cell [91]. The top panel shows a side view, and the bottom panel shows a view of the ventral region adjacent to the substratum (dashed region in the top view). The cell body is a passive cargo, but the perinuclear mitochondria generate an anterior–posterior pH gradient which regulates gelation and solation of the MSP gel in the lamellipod. At the (basic) leading edge, the growing MSP filaments bundle into thick fibers. This bundling extends the filaments beyond their equilibrium length pushing the cell front out, and at the same time storing elastic energy. In the acidic environment at the rear, the inter-filament interactions weaken, and the filaments unbundle and entropically contract to their equilibrium length. This provides the contractile force to pull up the cell body.

to the size of an actin monomer. These steps could suggest some intrinsic molecular scale mechanism at the interface between filaments and the surface. More research is required to clarify the relation of these microscopic models to the elastic polymerization ratchet mechanism.

Finally, myosin is involved in some way during protrusion of filopodia [80]. Filopodial-like actin bundles can be organized by inhibition of capping and subsequent cross-linking by fascin at the lamellipodial leading edge [81]. The transition between orthogonal networks of semi-stiff polymers and cross-linked bundles may arise as a phase transition that depends only on the concentration of cross-links, not on their detailed properties (A. Liu, personal communication). If verified *in vivo*, this may provide another mechanism for force production analogous to the bundling pressure in nematode sperm locomotion (see below).

A complete macroscopic model of forces and movements in cell protrusion is still pending. However, an important advance was achieved by Gerbal *et al.* [82] who constructed a continuum model of *Listeria* propulsion based on the elastic shear stress developed by growth of the actin meshwork at the cell surface. In this model, the polymerization of actin develops circumferential stresses in the actin meshwork of the tail surrounding the posterior portion of the cell. This developing stress 'squeezes' the cell until a yield stress is reached, whereupon the cell 'squirts' forward, relieving the stress, and the cycle repeats. This stress–relaxation cycle produces step-like propulsion — with micron-sized steps — similar to that observed in the movement of ActA-coated plastic beads [83]. Being macroscopic, this model complements the microscopic elastic ratchet model; indeed, the latter provides a rationale for the polymerization induced stresses that develop in the continuum gel model.

Lipid vesicles coated with ActA also grow actin tails and move. The vesicles deform, and the stress distribution exerted by the actin can be computed from their shape [84]. These experiments confirm the existence of large (~nN) 'squeezing' stresses on the vesicle, but 'squirting' movement cycles were not observed. These experiments also indicate that a spatial separation between tethered and working filaments develops: tethered filaments are swept to the very rear of the vesicle, while working filaments concentrate at the sides. A simple explanation for this separation phenomenon could be that ActA attached to an immobile tethered filament drifts to the rear along the lipid surface as the vesicle is propelled forward by working filaments that keep up with the vesicle's sides.

Other bead experiments revealed that, after polymerizing a dense actin network around itself, the bead would frequently 'break through' the actin meshwork and propel itself directionally, forming an actin mesh tail [58]. A Brownian ratchet theory that incorporates a force-dependent actin depolymerization to generate instability explains the onset of the 'breaking through' stage [85]. A full explanation of this

Box 2

Disassembly-Induced Contraction in Gels.

As discussed in the text, the actin cytoskeleton comprises an osmotically swollen polyelectrolyte gel. At equilibrium, the elastic tension in the gel filaments just counterbalances the osmotic pressure of the gel counterions. Here we give some estimates of the forces of expansion and contraction that determine the shape of an actin or MSP gel.

The entropic contraction force that can be generated by one semi-stiff filament can be estimated as follows. Consider the filament connecting two cross-links in the gel. Its transverse thermal fluctuations tend to pull the cross-links together. The equilibrium distance between the ends of a thermally fluctuating elastic rod of length L is ~$L - L^2/6\lambda$, where $\lambda >> L$ is the thermal *persistence length*, related to the bending modulus, B, by $\lambda \approx k_BT/B$ [8]. If the filament is heavily cross-linked in a stress-free state, its length is L; if the cross-links are removed, the filament deforms by about $L^2/6\lambda$. The effective spring constant of such undulating filament is ~10 $k_BT\lambda^2/L^4$ [23]. The contraction force of an actin filament of length 200 nm with persistence length 10 μm is ~ $k_BT\lambda/L^2$ ~4 pN. Thus, each filament is able to generate contraction force in the pN range.

Next, consider the isotropic expansion of a sphere of a gel made of very flexible filaments, so that their persistence length is less than the average distance between cross-links, $\lambda << L$. All physiologically relevant cytoskeletal gels have a volume fraction, ϕ = (gel volume)/(gel + fluid volume) smaller than ~0.1. In this limit, the entropic part of the free energy of 'mixing' the filaments with liquid and the inter-polymer interactions are negligible in comparison with the elastic and counterion parts of the gel free energy. Therefore, the swelling pressure tending to expand the gel is the difference between the counterion pressure and the restraining elastic pressure $P_{swell} = P_{osm} - P_{elas}$. The osmotic pressure, when the bath molar ion concentration is very low, is $P_{osm} \approx (k_BT/v)\ \alpha\phi$, where v is the monomer volume, and α is charge per monomer [96]. That is the osmotic pressure is just the van't Hoff's law: $P_{osm} = k_BTc$, where $c = \alpha\phi/v$ is the counterion concentration. Thus the counterion pressure can be viewed as a nearly ideal gas tending to expand the gel. The elastic pressure is $P_{elas} \approx (k_BT/v)(\phi_0/N_c)[(\phi/2\phi_0) - (\phi/\phi_0)^{1/3}]$ [96,111,112]. Here N_c is the average number of monomers between adjacent cross-links, and ϕ is the volume fraction at which the gel is in the elastic stress-free state. The osmotic pressure tends to expand the gel so that its volume fraction falls below ϕ; thus the gel filaments are under tension. At equilibrium, this elastic tension balances the osmotic pressure of the counterion gas, which is in compression. The order of magnitude of both elastic, and osmotic pressure is $P \sim (k_BT/v)\cdot\alpha\phi \sim (k_BT/v)(\phi/N_c) \sim 10^3$ [pN/μm^2], where α ~ 0.1, N_c ~10, ϕ ~0.1, v ~50 nm^3. If the cross-links are partially removed — the gel partially 'solates' — the parameter N_c increases and the elasticity of the gel weakens, allowing the osmotic pressure to expand the gel to a larger volume (Figure 5). The force of expansion is in the range of hundreds of pN per square micron, and the expansion would take but a few tenths of a second for a micron sized ball.

Our estimates above assume that the gels consist of very flexible filaments, like MSP polymers. Highly entangled and cross-linked s*emi-stiff* actin networks have a much more complex behavior [113]. Their viscoelasticity is characterized by large elastic moduli that are very sensitive to polymer lengths and concentrations of actin and cross-links. Moreover, such networks have complex (and sometimes conflicting) properties of strain hardening and thixotropy that allow them to flow only at large stresses. Despite these complexities, our simple estimate of stress and deformation of one cross-linked filament above shows that cross-linking leads to gel swelling, while solating cross-links causes contraction with forces in the range found in lamellipodia. Note that this behavior of semi-stiff gels is opposite to that of the rubber-like gels, where cross-linking leads to contraction and solation causes expansion. This illustrates the extremely complex and diverse character of the physics of gels that may have important implications for cell movements.

It is interesting to note that macroscopic cyclical engines based on entropic contraction of polyelectrolytes were designed and built by Katchalsky and his coworkers [114,115] long before many of the cellular counterparts were discovered. These prescient papers are still worth reading for they explain the basic physics underlying the operation of the motors discussed here.

phenomenon, however, will require modeling the elasticity and fracture of the actin gel.

Turning back to the question of how cells push out their front, several mechanisms other than polymerization are probably operating in certain systems. In most crawling cells, the force of protrusion is generated locally [86]. Localized protrusive forces can be generated in actin gels because they are highly charged [87]. Because of the counterions to the actin fixed charges, the filaments of a cross-linked polyelectrolyte gel, such as the actin cytoskeletal network, are always in a state of elastic tension. At equilibrium, the elastic tension in the gel filaments is just balanced by the ion osmotic pressure. This is discussed in more detail in Box 2, where we give some estimates of the forces involved. In transiently motile cells, the actin gel adjacent to the leading edge membrane may partially solate, for example, by the action of severing proteins like gelsolin triggered by calcium influx. This weakens elasticity of the gel so that the *local* osmotic pressure expands the gel boundary to a new equilibrium. Subsequently, the gel solidifies again stabilizing the protrusion. Some indirect evidence in favor of this scenario are the observations that raising external osmolarity inhibits protrusion, and that prior to protrusion, the lamellipodial leading edge of some cells swells and becomes softer [88].

A very simple and specialized cell, the nematode sperm of *Ascaris suum*, provides an important example of pushing out the front by a peculiar form of gel swelling (Figure 4). In these cells, the locomotion machinery is dramatically simplified. Nematode sperm lack the actin machinery typically associated with amoeboid cell motility; instead, their movement is powered by a cytoskeleton built from filaments of the major sperm protein (MSP) [89]. MSP is a positively charged and partially hydrophobic protein which associates into symmetrical dimers that polymerize into helical filaments. Unlike actin, MSP polymerization and bundling does not require a broad spectrum of accessory proteins. The same hydrophobic and electrostatic interaction interfaces allow these filaments to wind together in pairs to form larger bundles, and eventually congregate into higher-order rope-like arrays [90].

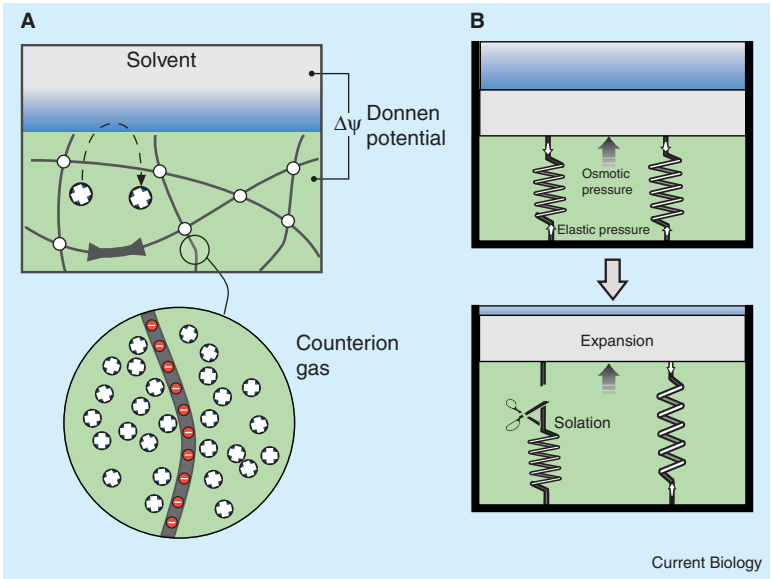

Figure 5. Force generation in polyelectrolyte gels.
(A) Negatively charged filaments are surrounded by positive counterions that are confined inside gel by the Donnen (diffusion) potential. Therefore, they exert a gas-like swelling pressure that is resisted by the elastic contractile forces developed by the expanded, cross-linked, and entangled flexible filaments. (B) Partial solation of the gel decreases the effective rigidity of the polymer mesh allowing the osmotic pressure to expand the gel.

MSP filaments are more flexible than actin, and so the polymerization ratchet mechanism may not be as effective in generating a protrusive force in nematode sperm. However, this assembly process forces the filaments within a higher-order aggregate to assume an end-to-end distance that is larger than its persistence length in solution (compare with Box 1). In this fashion, bundles of MSP filaments are stiffer than, and contain the stored elastic energy of, their constituent filaments. These bundles of MSP form a thixotropic (shear-thining) gel-like cytoskeleton within the lamellipod. This gel is a fibrous material, so that when filaments bundle laterally they generate a protrusive force longitudinally — the so-called Poisson expansion (see Figure 4 and [91]).

Pulling Up the Back

So far, we concentrated on the force of protrusion pushing out the front of the cell. Much less is known about the forces of contraction pulling up its rear. One of the favorite cells used to study this phenomenon is the fish keratocyte and its lamellipodial fragments [92,93]. In the proximal region of the lamellipod, the actin network is dense and highly cross-linked. As the leading edge extends, depolymerization begins to weaken the actin network. In the posterior lamellipod, the network is weakened enough for myosin clusters there to collapse the square lattice of actin filaments into bi-polar bundles of counter-oriented filaments that contract in a muscle-like fashion to pull the cell body forward and limit extension of the lamellipodial sides. The total traction force exerted by the cell is ~10^4–10^5 pN, which compares well with the total number (~10^4–10^5) of myosin molecules, each able to generate a few pN of force (reviewed in [74]).

Myosin-powered contraction may not be the whole story. A solating gel can generate entropic contractile forces of a few pN per filament, as explained in Box 2 [23]. This adds up to thousands of pN for a whole lamellipod, making this mechanism a viable supplement for myosin powered contraction. However, because actin gels are ‘semi-stiff’ [94], entropic contraction is unlikely to generate significant translocation of the cell rear. But the entropic contraction mechanism does appear to be involved in the crawling of nematode sperm that lack filament-based molecular motors, and whose cytoskeleton is composed of more flexible MSP filaments.

A model that explains the behavior of this odd cell operates by the following mechanism, illustrated in Figure 4 [91]. As the bundled MSP gel moves rearward, with respect to the leading edge, it encounters a rising proton concentration generated by the perinuclear mitochondria. The protons compete with the electrostatic cross-linking sites on MSP filaments and weaken the hydrophobic interactions as well. Weakening of the cohesive forces in the MSP filaments and bundles allows individual MSP filaments to dissociate from the fiber complexes. As they do so, they attempt to contract entropically to their equilibrium end-to-end length. This solation process releases the elastic energy in the gel, stored by bundling at the front, to generate a contractile stress. This model illustrates that, while there is much left to learn about contraction mechanisms, it is clear that cytoskeletal gels can not only contribute to pushing out the cell front, but also to pulling up its rear.

Molecular Springs and Ratchets

There are many other fascinating examples of nature’s resourcefulness in using dynamic cytoskeletal fibers to generate force. Here are just a few of them. ATP-dependent polymerization of actin-like filaments appears to generate the force for the directional movement of plasmids to opposite cell poles in a simple prokaryotic analog of the eukaryotic mitotic spindle apparatus [95]. *Myxococcus xanthus* cells glide on surfaces by hydration and extrusion of a gel from nozzle-like organelles [96]. The smallest free-living organisms are the *Mollicutes* [97]. Some glide on surfaces, others swim, but all appear to generate the forces for propulsion by cyclically altering the elastic properties of cytoplasmic filaments [98–100].

At the other end of the spectrum, the largest and fastest reversible entropic motor is employed by spasmoneme in *Vorticellid* ciliates [101]. In this motor, a giant polymer chain is held in a distended configuration by the repulsion of its fixed charges. A rise in cytosolic calcium drastically reduces its rigidity by shielding the polymer-associated charges, triggering a strong entropic contractile force (similar to the mechanism described in Box 2). Another dramatically fast 'one-shot' polymerization engine is employed when the sperm of the sea cucumber *Thyone* encounters the egg jelly coat. An explosive actin polymerization reaction ensues, pushing out the acrosomal process and enabling the sperm plasma membrane to penetrate the egg and fuse with the plasma membrane of the egg [102]. In this process, fast and transient actin polymerization is limited by actin delivery to the tip of the process, rather than by force. Water influx coupled with actin polymerization may contribute to force generation by a hydrostatic mechanism [103]. Note that this phenomenon is an example of a polymerization motor that works without treadmilling and/or hydrolysis. The acrosomal process of the *Limulus* sperm stores elastic energy by using the actin-binding protein scruin to trap thermal fluctuations during polymerization as elastic strain energy in the actin filament. Later, this strain energy is released to generate the force required to push the actin rod into the egg cortex [7].

Future Directions

It should be clear from this review that, beyond polymerization of single filaments, our knowledge is sketchy about how forces are generated by assembling or disassembling cytoskeletal fibers and networks. Even cloudier is the issue of how these forces organize themselves, using complementary and antagonistic actions of microtubules and actin, coupled with plus and minus directed motors, to drive motile and dividing cells. These problems offer opportunities for new models to stimulate new experiments in the physics and biology of cell movements. Any cellular process involving more than a few types of molecule is too complicated to understand without a mathematical model to expose assumptions and to frame the qualitative picture in quantitative terms. Moreover, force generation is intimately tied in with the processes of regulation [3], signal transduction [104], adhesion [105] and many other aspects of cell dynamics. These are exciting times for students of cell mechanics.

Acknowledgments

We apologize for not citing every colleague's work due to space limitations of this article. We thank T. Pollard and M. Dogterom for useful comments on the manuscript. A.M. was supported by NSF Grant DMS-0073828. G.O. was supported by National Institutes of Health grant GM59875-02.

References

1. Abercrombie, M. (1980). The Croonian lecture, 1978. The crawling movement of metazoan cells. Proc. R. Soc. Lond. B. Biol. Sci. *207*, 129–147.
2. Bray, D. (2002). Cell Movements (New York: Garland).
3. Pollard, T.D., and Borisy, G.G. (2003). Cellular motility driven by assembly and disassembly of actin filaments. Cell *112*, 453–465.
4. Theriot, J.A. (2000). The polymerization motor. Traffic *1*, 19–28.
5. Inoue, S., and Salmon, E.D. (1995). Force generation by microtubule assembly/disassembly in mitosis and related movements. Mol. Biol. Cell *6*, 1619–1640.
6. Howard, J., and Hyman, A.A. (2003). Dynamics and mechanics of the microtubule plus end. Nature *422*, 753–758.
7. Mahadevan, L., and Matsudaira, P. (2000). Motility powered by supramolecular springs and ratchets. Science *288*, 95–100.
8. Howard, J. (2001). Mechanics of Motor Proteins and the Cytoskeleton (Sunderland, MA: Sinauer).
9. Pollack, G. (2001). Cells, Gels and the Engines of Life (Seattle: Ebner & Sons).
10. Boal, D. (2002). Mechanics of the Cell (Cambridge: Cambridge University Press).
11. Mogilner, A., Elston, T., Wang, H.-Y., and Oster, G. (2002). Molecular motors: Theory and examples. In Computational Cell Biology. C. Fall, E. Marland, J. Tyson, J. Wagner, eds (NY: Springer), pp. 321–380.
12. Oster, G., and Wang, H. (2003). Rotary protein motors. Trends Cell Biol. *13*, 114–121.
13. Schliwa, M. ed. (2002). Molecular Motors (Weinheim: Wiley-VCH).
14. Oster, G. (2002). Brownian ratchets: Darwin's motors. Nature *417*, 25.
15. Hill, T., and Kirschner, M. (1982). Bioenergetics and kinetics of microtubule and actin filament assembly and disassembly. Int. Rev. Cytol. *78*, 1–125.
16. Cortese, J.D., Schwab, B., 3rd, Frieden, C., and Elson, E.L. (1989). Actin polymerization induces a shape change in actin-containing vesicles. Proc. Natl. Acad. Sci. USA *86*, 5773–5777.
17. Miyata, H., and Hotani, H. (1992). Morphological changes in liposomes caused by polymerization of encapsulated actin and spontaneous formation of actin bundles. Proc. Natl. Acad. Sci. USA *89*, 11547–11551.
18. Honda, M., Takiguchi, K., Ishikawa, S., and Hotani, H. (1999). Morphogenesis of liposomes encapsulating actin depends on the type of actin-cross-linking. J. Mol. Biol. *287*, 293–300.
19. Condeelis, J. (1993). Life at the leading edge: the formation of cell protrusions. Annu. Rev. Cell Biol. *9*, 411–444.
20. Peskin, C.S., Odell, G.M., and Oster, G. (1993). Cellular motions and thermal fluctuations: the Brownian ratchet. Biophys. J. *65*, 316–324.
21. Feynman, R., Leighton, R., and Sands, M. (1963). The Feynman Lectures on Physics, Volume 1 (Reading, MA: Addison-Wesley).
22. Wang, H., and Oster, G. (2001). Ratchets, power strokes, and molecular motors. Appl. Phys. A *75*, 315–323.
23. Mogilner, A., and Oster, G. (1996). The physics of lamellipodial protrusion. Eur. Biophys. J. *25*, 47–53.
24. Mogilner, A., and Oster, G. (1996). Cell motility driven by actin polymerization. Biophys. J. *71*, 3030–3045.
25. Mogilner, A., and Oster, G. (1999). The polymerization ratchet model explains the force-velocity relation for growing microtubules. Eur. J. Biophys. *28*, 235–242.
26. Mogilner, A., and Oster, G. (2003). Force generation by actin polymerization II: the elastic ratchet and tethered filaments. Biophys. J. *84*, 1591–1605.
27. Pollard, T., Blanchoin, L., and Mullins, R. (2001). Actin dynamics. J. Cell Sci. *114*, 3–4.
28. Miyata, H., Nishiyama, S., Akashi, K., and Kinosita, K., Jr. (1999). Protrusive growth from giant liposomes driven by actin polymerization. Proc. Natl. Acad. Sci. USA *96*, 2048–2053.
29. Dogterom, M., and Yurke, B. (1997). Measurement of the force-velocity relation for growing microtubules. Science *278*, 856–860.
30. van Doorn, G.S., Tanase, C., Mulder, B.M., and Dogterom, M. (2000). On the stall force for growing microtubules. Eur. Biophys. J. *29*, 2–6.
31. Hotani, H., and Miyamoto, H. (1990). Dynamic features of microtubules as visualized by dark-field microscopy. Adv. Biophys. *26*, 135–156.
32. Fygenson, D., Marko, J., and Libchaber, A. (1997). Mechanics of microtubule-based membrane extension. Phys. Rev. Lett. *79*, 4497–4500.
33. McIntosh, J.R., and Pfarr, C.M. (1991). Mitotic motors. J. Cell Biol. *115*, 577–585.
34. Barton, N.R., and Goldstein, L.S. (1996). Going mobile: microtubule motors and chromosome segregation. Proc. Natl. Acad. Sci. USA *93*, 1735–1742.

35. Tran, P.T., Marsh, L., Doye, V., Inoue, S., and Chang, F. (2001). A mechanism for nuclear positioning in fission yeast based on microtubule pushing. J. Cell Biol. *153*, 397–411.

36. Cassimeris, L., Rieder, C.L., and Salmon, E.D. (1994). Microtubule assembly and kinetochore directional instability in vertebrate monopolar spindles: implications for the mechanism of chromosome congression. J. Cell Sci. *107*, 285–297.

37. Brunet, S., and Vernos, I. (2001). Chromosome motors on the move. From motion to spindle checkpoint activity. EMBO Rep. *2*, 669–673.

38. Cytrynbaum, E.N., Scholey, J.M., and Mogilner, A. (2003). A force balance model of early spindle pole separation in Drosophila embryos. Biophys. J. *84*, 757–769.

39. Coue, M., Lombillo, V.A., and McIntosh, J.R. (1991). Microtubule depolymerization promotes particle and chromosome movement *in vitro*. J. Cell Biol. *112*, 1165–1175.

40. Lombillo, V.A., Stewart, R.J., and McIntosh, J.R. (1995). Minus-end-directed motion of kinesin-coated microspheres driven by microtubule depolymerization. Nature *373*, 161–164.

41. Desai, A., Verma, S., Mitchison, T.J., and Walczak, C.E. (1999). Kin I kinesins are microtubule-destabilizing enzymes. Cell *96*, 69–78.

42. Lombillo, V.A., Nislow, C., Yen, T.J., Gelfand, V.I., and McIntosh, J.R. (1995). Antibodies to the kinesin motor domain and CENP-E inhibit microtubule depolymerization-dependent motion of chromosomes *in vitro*. J. Cell Biol. *128*, 107–115.

43. Hill, T.L. (1985). Theoretical problems related to the attachment of microtubules to kinetochores. Proc. Natl. Acad. Sci. USA *82*, 4404–4408.

44. Joglekar, A.P., and Hunt, A.J. (2002). A simple, mechanistic model for directional instability during mitotic chromosome movements. Biophys. J. *83*, 42–58.

45. Wang, M.D., Schnitzer, M.J., Yin, H., Landick, R., Gelles, J., and Block, S.M. (1998). Force and velocity measured for single molecules of RNA polymerase. Science *282*, 902–907.

46. Mitchison, T.J. (1988). Microtubule dynamics and kinetochore function in mitosis. Annu. Rev. Cell Biol. *4*, 527–549.

47. Arnal, I., Karsenti, E., and Hyman, A.A. (2000). Structural transitions at microtubule ends correlate with their dynamic properties in Xenopus egg extracts. J. Cell Biol. *149*, 767–774.

48. Hyman, A.A., Chretien, D., Arnal, I., and Wade, R.H. (1995). Structural changes accompanying GTP hydrolysis in microtubules: information from a slowly hydrolyzable analogue guanylyl-(α,β)-methylene-diphosphonate. J. Cell Biol. *128*, 117–125.

49. Peskin, C.S., and Oster, G.F. (1995). Force production by depolymerizing microtubules: load-velocity curves and run-pause statistics. Biophys. J. *69*, 2268–2276.

50. Tao, Y.C., and Peskin, C.S. (1998). Simulating the role of microtubules in depolymerization-driven transport: a Monte Carlo approach. Biophys. J. *75*, 1529–1540.

51. Scholey, J.M., and Mogilner, A. (2002). Mitotic spindle motors. In Molecular Motors, M. Schliwa, ed. (Berlin: Wiley-VCH), pp. 327–355.

52. Alexander, S.P., and Rieder, C.L. (1991). Chromosome motion during attachment to the vertebrate spindle: initial saltatory-like behavior of chromosomes and quantitative analysis of force production by nascent kinetochore fibers. J. Cell Biol. *113*, 805–815.

53. Nicklas, R.B. (1983). Measurements of the force produced by the mitotic spindle in anaphase. J. Cell Biol. *97*, 542–548.

54. Liakopoulos, D., Kusch, J., Grava, S., Vogel, J., and Barral, Y. (2003). Asymmetric loading of Kar9 onto spindle poles and microtubules ensures proper spindle alignment. Cell *112*, 561–574.

55. Tilney, L.G., and Portnoy, D.A. (1989). Actin filaments and the growth, movement, and spread of the intracellular bacterial parasite, *Listeria monocytogenes*. J. Cell Biol. *109*, 1597–1608.

56. Cameron, L.A., Svitkina, T.M., Vignjevic, D., Theriot, J.A., and Borisy, G.G. (2001). Dendritic organization of actin comet tails. Curr. Biol. *11*, 130–135.

57. Theriot, J.A., Mitchison, T.J., Tilney, L.G., and Portnoy, D.A. (1992). The rate of actin-based motility of intracellular *Listeria monocytogenes* equals the rate of actin polymerization. Nature *357*, 257–260.

58. Cameron, L.A., Footer, M.J., van Oudenaarden, A., and Theriot, J.A. (1999). Motility of ActA protein-coated microspheres driven by actin polymerization. Proc. Natl. Acad. Sci. USA *96*, 4908–4913.

59. Loisel, T.P., Boujemaa, R., Pantaloni, D., and Carlier, M.F. (1999). Reconstitution of actin-based motility of Listeria and Shigella using pure proteins. Nature *401*, 613–616.

60. Cameron, L.A., Giardini, P.A., Soo, F.S., and Theriot, J.A. (2000). Secrets of actin-based motility revealed by a bacterial pathogen. Nat. Rev. Mol. Cell Biol. *1*, 110–119.

61. Pantaloni, D., Le Clainche, C., and Carlier, M.F. (2001). Mechanism of actin-based motility. Science *292*, 1502–1506.

62. Winder, S.J. (2003). Structural insights into actin-binding, branching and bundling proteins. Curr. Opin. Cell Biol. *15*, 14–22.

63. Weaver, A.M., Young, M.E., Lee, W.-L., and Cooper, J.A. (2003). Integration of signals to the Arp2/3 complex. Curr. Opin. Cell Biol. *15*, 23–30.

64. Noireaux, V., Golsteyn, R.M., Friederich, E., Prost, J., Antony, C., Louvard, D., and Sykes, C. (2000). Growing an actin gel on spherical surfaces. Biophys. J. *78*, 1643–1654.

65. Kuo, S.C., and McGrath, J.L. (2000). Steps and fluctuations of *Listeria monocytogenes* during actin-based motility. Nature *407*, 1026–1029.

66. McGrath, J.L., Eungdamrong, N.J., Fisher, C.I., Peng, F., Mahadevan, L., Mitchison, T.J., and Kuo, S.C. (2003). The force-velocity relationship for the actin-based motility of *Listeria monocytogenes*. Curr. Biol. *13*, 329–332.

67. Wiesner, S., Helfer, E., Didry, D., Ducouret, G., Lafuma, F., Carlier, M.F., and Pantaloni, D. (2003). A biomimetic motility assay provides insight into the mechanism of actin-based motility. J. Cell Biol. *160*, 387–398.

68. Goldberg, M.B. (2001). Actin-based motility of intracellular microbial pathogens. Microbiol. Mol. Biol. Rev. *65*, 595–626.

69. Upadhyaya, A., Chabot, J.R., Andreeva, A., Samadani, A., and Van Oudenaarden, A. (2003). Probing polymerization forces by using actin-propelled lipid vesicles. Proc. Natl. Acad. Sci. USA *100*, 4521–4526.

70. Abraham, V.C., Krishnamurthi, V., Taylor, D.L., and Lanni, F. (1999). The actin-based nanomachine at the leading edge of migrating cells. Biophys. J. *77*, 1721–1732.

71. Maly, I.V., and Borisy, G.G. (2001). Self-organization of a propulsive actin network as an evolutionary process. Proc. Natl. Acad. Sci. USA *98*, 11324–11329.

72. Small, J.V., Herzog, M., and Anderson, K. (1995). Actin filament organization in the fish keratocyte lamellipodium. J. Cell Biol. *129*, 1275–1286.

73. Mogilner, A., and Edelstein-Keshet, L. (2002). Regulation of actin dynamics in rapidly moving cells: a quantitative analysis. Biophys. J. *83*, 1237–1258.

74. Oliver, T., Lee, J., and Jacobson, K. (1994). Forces exerted by locomoting cells. Semin. Cell Biol. *5*, 139–147.

75. Evans, E., and Yeung, A. (1989). Apparent viscosity and cortical tension of blood granulocytes determined by micropipet aspiration. Biophys. J. *56*, 151–160.

76. Dai, J.W., and Sheetz, M.P. (1999). Membrane tether formation from blebbing cells. Biophys. J. *77*, 3363–3370.

77. Bear, J.E., Svitkina, T.M., Krause, M., Schafer, D.A., Loureiro, J.J., Strasser, G.A., Maly, I.V., Chaga, O.Y., Cooper, J.A., Borisy, G.G., Gertler, F.B. (2002). Antagonism between Ena/VASP proteins and actin filament capping regulates fibroblast motility. Cell *109*, 509–521.

78. Laurent, V., Loisel, T.P., Harbeck, B., Wehman, A., Grobe, L., Jockusch, B.M., Wehland, J., Gertler, F.B., and Carlier, M.F. (1999). Role of proteins of the Ena/VASP family in actin-based motility of Listeria monocytogenes. J. Cell Biol. *144*, 1245–1258.

79. Dickinson, R.B., and Purich, D.L. (2002). Clamped-filament elongation model for actin-based motors. Biophys. J. *82*, 605–617.

80. Sheetz, M.P., Wayne, D.B., and Pearlman, A.L. (1992). Extension of filopodia by motor-dependent actin assembly. Cell Motil. Cytoskeleton *22*, 160–169.

81. Vignjevic, D., Yarar, D., Welch, M.D., Peloquin, J., Svitkina, T., and Borisy, G.G. (2003). Formation of filopodia-like bundles *in vitro* from a dendritic network. J. Cell Biol. *160*, 951–962.

82. Gerbal, F., Chaikin, P., Rabin, Y., and Prost, J. (2000). An elastic analysis of *Listeria monocytogenes* propulsion. Biophys. J. *79*, 2259–2275.

83. Bernheim-Groswasser, A., Wiesner, S., Golsteyn, R.M., Carlier, M.F., and Sykes, C. (2002). The dynamics of actin-based motility depend on surface parameters. Nature *417*, 308–311.

84. Giardini, P.A., Fletcher, D.A., and Theriot, J.A. (2003). Compression forces generated by actin comet tails on lipid vesicles. Proc. Natl. Acad. Sci. USA *100*, 6493–6498.

85. van Oudenaarden, A., and Theriot, J.A. (1999). Cooperative symmetry-breaking by actin polymerization in a model for cell motility. Nat. Cell Biol. *1*, 493–499.

86. Grebecki, A. (1994). Membrane and cytoskeleton flow in motile cells with emphasis on the contribution of free-living amoebae. Int. Rev. Cytol. *148*, 37–80.

87. Oster, G.F. (1984). On the crawling of cells. J. Embryol. Exp. Morphol. *83* (*Suppl*), 329–364.

88. Rotsch, C., Jacobson, K., Condeelis, J., and Radmacher, M. (2001). EGF-stimulated lamellipod extension in adenocarcinoma cells. Ultramicroscopy *86*, 97–106.

89. Italiano, J.E., Jr., Stewart, M., and Roberts, T.M. (2001). How the assembly dynamics of the nematode major sperm protein generate amoeboid cell motility. Int. Rev. Cytol. *202*, 1–34.

90. Roberts, T.M., Salmon, E.D., and Stewart, M. (1998). Hydrostatic pressure shows that lamellipodial motility in Ascaris sperm requires membrane-associated major sperm protein filament nucleation and elongation. J. Cell Biol. *140*, 367–375.

91. Bottino, D., Mogilner, A., Roberts, T., Stewart, M., and Oster, G. (2002). How nematode sperm crawl. J. Cell Sci. *115*, 367–384.

92. Svitkina, T.M., Verkhovsky, A.B., McQuade, K.M., and Borisy, G.G. (1997). Analysis of the actin-myosin II system in fish epidermal keratocytes: mechanism of cell body translocation. J. Cell Biol. *139*, 397–415.

93. Verkhovsky, A.B., Svitkina, T.M., and Borisy, G.G. (1999). Self-polarization and directional motility of cytoplasm. Curr. Biol. *9*, 11–20.

94. Janmey, P.A., Hvidt, S., Kas, J., Lerche, D., Maggs, A., Sackmann, E., Schliwa, M., and Stossel, T.P. (1994). The mechanical properties of actin gels. Elastic modulus and filament motions. J. Biol. Chem. *269*, 32503–32513.

95. Moller-Jensen, J., Jensen, R.B., Lowe, J., and Gerdes, K. (2002). Prokaryotic DNA segregation by an actin-like filament. EMBO J. *21*, 3119–3127.

96. Wolgemuth, C., Hoiczyk, E., Kaiser, D., and Oster, G. (2002). How myxobacteria glide. Curr. Biol. *12*, 369–377.

97. Trachtenberg, S. (1998). Mollicutes-Wall-less bacteria with internal cytoskeletons. J. Struct. Biol. *124*, 244–256.

98. Wolgemuth, C., Igoshin, O., and Oster, G. (2003). The motility of Mollicutes. Biophys. J., in press.

99. Trachtenberg, S., Gilad, R., and Geffen, N. (2003). The bacterial linear motor of *Spiroplasma melliferum* BC3: from single molecules to swimming cells. Mol. Microbiol. *47*, 671–697.

100. Trachtenberg, S., and Gilad, R. (2001). A bacterial linear motor: cellular and molecular organization of the contractile cytoskeleton of the helical bacterium spiroplasma melliferum BC3. Mol. Microbiol. *41*, 827–848.

101. Moriyama, Y., Okamoto, H., and Asai, H. (1999). Rubber-like elasticity and volume changes in the isolated spasmoneme of giant Zoothamnium sp. under Ca^{2+}-induced contraction. Biophys. J. *76*, 993–1000.

102. Tilney, L.G., and Inoue, S. (1982). Acrosomal reaction of Thyone sperm. II. The kinetics and possible mechanism of acrosomal process elongation. J. Cell Biol. *93*, 820–827.

103. Oster, G., Perelson, A., and Tilney, L. (1982). A mechanical model for acrosomal extension in *Thyone.* J. Math. Biol. *15*, 259–265.

104. Bourne, H., and Weiner, O. (2002). A chemical compass. Nature *419*, 21.

105. Webb, D.J., Parsons, J.T., and Horwitz, A.F. (2002). Adhesion assembly, disassembly and turnover in migrating cells - over and over and over again. Nat. Cell Biol. *4*, E97–100.

106. Bustamante, C., Keller, D., and Oster, G. (2001). The physics of molecular motors. Acc. Chem. Res. *34*, 412–420.

107. Oster, G., and Wang, H. (2000). Reverse engineering a protein: The mechanochemistry of ATP synthase. Biochim. Biophys. Acta *1458*, 482–510.

108. Visscher, K., Schnitzer, M.J., and Block, S.M. (1999). Single kinesin molecules studied with a molecular force clamp. Nature *400*, 184–189.

109. Ruegg, C., Veigel, C., Molloy, J.E., Schmitz, S., Sparrow, J.C., and Fink, R.H. (2002). Molecular motors: force and movement generated by single myosin II molecules. News Physiol. Sci. *17*, 213–218.

110. Biggins, S., and Walczak, C.E. (2003). Captivating capture: how microtubules attach to kinetochores. Curr. Biol. *13*, R449–R460.

111. Hill, T. (1960). Introduction to Statistical Thermodynamics (Reading MA: Addison Wesley).

112. Dill, K., and Bromberg, S. (2003). Molecular Driving Forces: Statistical Thermodynamics in Chemistry and Biology (New York: Garland).

113. MacKintosh, F.C., Kas, J., and Janmey, P.A. (1995). Elasticity of semiflexible biopolymer networks. Phys. Rev. Lett. *75*, 4425–4428.

114. Katchalsky, A., and Zwick, M. (1955). Mechanochemistry and ion exchange. J. Polym. Sci. *16*, 221–234.

115. Steinberg, I., Oplatka, A., and Katchalsky, A. (1966). Mechanochemical Engines. Nature *210*, 568–571.